A Novel Induction Machine Design Suitable for Inverter-DrivenVariable Speed Systems

Z. M. Zhao, *Senior Member, IEEE*, S. Meng, C. C. Chan, *Fellow, IEEE*, and E. W. C. Lo, *Member, IEEE*

***Abstract*—Induction machines designed for inverter-driven variable speed systems are different from those fed directly from a utility power line. In this paper, a novel design approach for inverter driven induction machines is presented and implemented. This is followed by an investigation on sizing equations and rotor slot shape specifically for this purpose. The proposed approach permits the integration of the design of machines with inverters, comprehensive performance analysis, and system optimization, resulting in 20–30% higher power density for the induction machine than those designed for direct utility power supplies by conventional methods. Simulation analysis and experimental results are presented to substantiate the conclusions.**

***Index Terms*—Induction machine design, inverter drive, variable speed.**

I. Introduction

INVERTER-DRIVEN induction machines (IDIM) are the prime choice of variable speed drives in a wide field of applications due to their low cost, simple and rugged construction, high reliability, minor maintenance, and well developed control algorithms [1]. Before the 1990s, however, the major attention had been given to the development of solid-state inverters and control algorithms, and the induction machines themselves had not gone through any profound changes compared to the solid-state inverter counterpart within the same system. Thus, the variable speed systems, particularly, high-speed drives and large machines still have the problems of low power factor, low efficiency and poor utilization of the inverter. In fact, with the inverter as the power supply, the operational conditions of an induction machine are much different from the conventional supply with fixed voltage and frequency, which implies that the design of induction machines should be reconsidered to make them more suitable for the inverter-driven variable speed systems.

Since the early 1990s, more attention has been given to the area and in 1991 an IEEE special task force was organized to investigate the needs for industrial standards for AC induction motors intended for use with adjustable-frequency controller [1]. The work reported in [2], [3] studied the influence of load and rotor slot design on harmonic losses of inverter-fed induction motors by finite element analysis. A design strategy for an IDIM has also been proposed in [4], [5] and corresponding computer aided design package was developed for maximizing the efficiency and improving the power factor [5]. Furthermore, optimization of the geometry of the rotor slot for cage induction motors has led to reduced harmonic losses [6] and static airgap eccentricity [7]. The work of [8] discussed the design and analysis of the inverter fed high speed cage induction motors for good efficiency, high torque performance, and wide speed range. However, most of the work done mainly has a focus on the negative impacts of an inverter on the induction machine, such as high switch frequency, harmonics, high voltage pulse, etc. As a matter of fact, the inverter drive also provides plenty of positive effects to the machine, such as variable frequency, vector control, minimum slip control and others, which benefit machine design very much.

In this paper, new design strategies of an IDIM are proposed and implemented, which make full use of the benefits from the inverter. First, the paper compares the operational conditions of an induction machine powered by an inverter, as opposed to those fed directly from commercial power lines. The design freedom gained by using an inverter is highlighted. Then, basic design strategies for an IDIM are explored. In particular, improved design equations are discussed to characterize the design and performance analysis of an IDIM. Based on these equations a computer aided design package is developed which is capable of designing and conducting electromagnetic, thermal and mechanical analysis for IDIM's. A family of parametric curves is then analyzed to illustrate the advantages of IDIM designs for a wide range of power ratings. Finally, a practical IDIM of 15 kW rating is constructed based on the proposed design strategies and the computer aided design package. Experimental results are given to detail the design and performance analysis of the IDIM as compared with that of a conventionally designed system.

II. Operation Conditions and Design Strategies

The operational conditions of an induction machine have to undergo a great change when it moves from the conventional supply to an inverter supply. The change of the mode of supply will not only influence the machine operation, but also the machine design.

A. Inverter-Driven Operating Conditions

The remarkable difference between the inverter supply and the utility line supply of an induction machine is that the former can change its frequency and input voltage flexibly, whereas the latter only provides a fixed frequency and voltage. With an adjustable frequency, an induction machine is able to move its torque-speed profile from the rated synchronous frequency to any other frequencies of interests as shown in Fig. 1.

Manuscript received March 3, 1999; revised April 7, 2000.

Z. M. Zhao and S. Meng are with the Department of Electrical Engineering, Tsinghua University, Beijing 100084, PR China.

C. C. Chan and E. W. C. Lo are with the Department of Electrical and Electronic Engineering, The University of Hong Kong, Hong Kong.

Publisher Item Identifier S 0885-8969(00)11001-0.

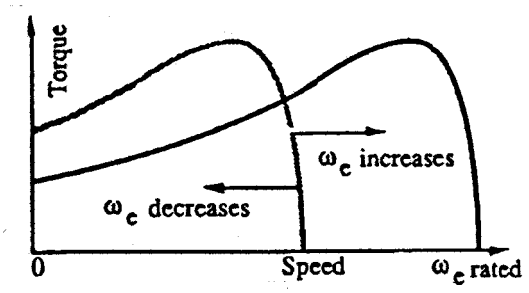

Fig. 1. Torque-speed in variable frequency operation.

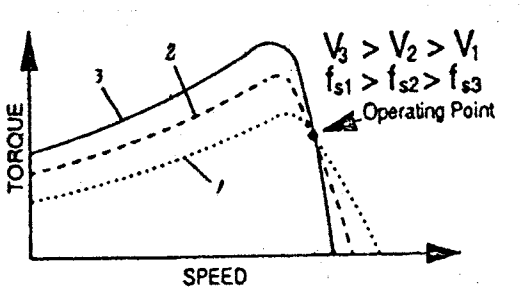

Fig. 2. Torque-speed curves with variable voltage and frequency.

This moveable torque-speed profile ensures that the line start-up performance of an induction machine under a fixed synchronous frequency and other considerations become unnecessary. Essentially, it is possible that the line-start torque can be replaced by the peak torque, and also the rated torque can be set at a most favorable slip frequency, resulting in a minimized slip power losses and stray iron losses. Reference [9] analyzed the situation as shown in Fig. 2. Fig. 2 shows a comparison for three torque-speed curves at different supply frequency and voltage. Obviously, a small operating slip frequency can be obtained by choosing a proper voltage V_3 and frequency f_3, thus a maximum efficiency can be achieved under the minimum slip control.

With an inverter as the power supply, an induction machine can be conveniently controlled with a field orientation scheme. In the rotor field oriented reference frame, the stator current of the induction machine can be decoupled into torque- and flux-producing components by a vector controller, and the flux-producing component can be minimized to enhance the power factor and efficiency of the machine.

B. Design Strategies

In a conventional design for commercial power lines, the basic considerations are: 1) to satisfy the required start-up characteristics; 2) to provide appropriate steady state characteristics, emphasizing efficiency and power factor; and 3) to permit easy and economic manufacturing. Items 1), 2) and 3) are generally assigned with weightings of 50%, 30% and 20%, respectively [4]. The conventional design strategy implies that in a standard induction machine design, the primary concern is the start-up characteristics, which include limiting inrush current, generating as much as possible starting torque, and ensuring a high starting efficiency. To meet the start-up requirements, the design strategy is searching for means to maximize the skin effect and to increase the rotor resistance during starting.

However, in designing an IDIM, the strategies are very different. Weighting assignments to Items 1) through 3) can be entirely changed because the two benefits are gained from the inverter supply, i.e. a) the start-up characteristics with a fixed frequency can be completely ignored; and b) the most favorable slip frequency can be selected to maximize efficiency. Thus, it is logical to assign all the design weighting to Items 2) and 3). Removing the weighting of Item 1) implies that restrictions imposed by rotor slot shape can also be lifted. The design with inverter driven condition allows the stator and rotor slot numbers, shapes, and size to be optimized exclusively for minimizing the leakage inductance and resistance. In general, the effective utilization of rotor slot area can be increased. Consequently, the advantages associated with the reduced rotor leakage inductance and resistance, such as increased peak torque, improved efficiency and power factor, can be expected.

The new design strategy has the potential to downsize the induction machine by about one or two frame size, without sacrificing its capacity and performance. This is because the design strategy based on inverter-driven conditions emphasizes the characteristics in variable frequency conditions rather than the fixed frequency start-up characteristics. In such a case, the inverter can control the induction machine so that it is operated always at a point close to the maximum torque, maximum efficiency and improved power factor. As a result, these maximums can be introduced to the sizing equations, in place of the starting torque, the conventionally defined rated efficiency and the power factor.

III. Major Design Equation and Improved Rotor Slot Shape

Many equations used for conventional induction machine design and analysis need modifications or new interpretation for inverter driven conditions and only those related to sizing the main dimensions and designing the rotor laminations are discussed here.

A. Main Dimensions

As all know, the sizing equation for main dimensions applied for conventional induction machines is in the form of

$$\frac{P_o}{n_s} = \xi D_i^2 l \tag{1}$$

The equation relates to the output power P_o, and the synchronous speed n_s to the rotor volume $D_i^2 l$, where D_i is the stator inner diameter and l the rotor effective length, through an output constant ξ which is expressed as follows

$$\xi = CB_g A\eta\cos\phi \tag{2}$$

where

B_g = flux density in airgap
A = surface current density in stator inner circle

C = machine constant
η = efficiency
$\cos\phi$ = power factor

Inspecting (1) and (2), it is seen that there are no relationships connecting these airgap quantities, B_g and A, with the flux and current densities existing in the machine's interior. In fact, machine size is affected by the complete stator geometry which includes the relative proportions of the stator inner and outer diameter, slot and tooth dimensions, flux densities in the iron parts and the actual current densities in conductors. In particular, with an inverter as the power supply, the flux and current usually contain some harmonics which directly affect the machine size. In order to consider the key factors, [10] presented a size equation as follows

$$\frac{P_o}{n_s} = f(\lambda) D_o^3 l \tag{3}$$

in which the inner diameter D_i and output constant ξ are replaced by stator outer diameter D_o and an output function $f(\lambda)$, respectively. $f(\lambda)$ is a function related to the ratio of inner to outer diameter of the stator. The $f(\lambda)$ can be expressed as below

$$f(\lambda) = C_1 B_g J_1 K_{cu} Q_1 K_w / K_e \eta \cos\phi (a\lambda^3 + b\lambda^2 + c\lambda) \tag{4}$$

C_1 is a constant,
J_1 is current density in stator slots,
K_{cu} the ratio of the conductor area to slot area,
Q_1 the number of stator slots,
K_w winding factor,
K_e voltage factor, and
λ is the ratio of inner to outer diameter of the stator.

The coefficients, a, b, and c, can be expressed as follows

$$a = \left[\frac{\pi}{Q_1 + \pi}(G_t + G_c)\right]^2 \left(\frac{Q_1}{4\pi} + \frac{\pi}{8}\right) - \left[\frac{\pi}{Q_1}(1 - G_t)\right]^2 \frac{Q_1}{4\pi}$$

$$b = -\left(\frac{\pi}{Q_1 + \pi}\right)^2 (G_t + G_c)\left(\frac{Q_1}{2\pi} + \frac{\pi}{4}\right)$$

$$c = \left(\frac{\pi}{Q + \pi}\right)^2 \left(\frac{Q_1}{4\pi} + \frac{\pi}{8}\right)$$

where G_t is the ratio of flux densities in the airgap and the stator teeth, and G_c the ratio of the flux density in the airgap and the stator core. As long as the coefficients, a, b and c, are determined, $f(\lambda)$ is a third-order function of λ. Therefore, a suitable value of λ can be figured out by solving the third order equation to obtain the maximum value of $f(\lambda)$, i.e., maximum output power.

Regarding to harmonic concerns, however, it is not enough by considering only the ratio of inner to outer diameter in designing a machine fed from an inverter. To solve this issue, a weighting related to the ratio of inverter's voltage harmonics and fundamental components is proposed:

$$\beta = \frac{1}{1 + \alpha} \tag{5}$$

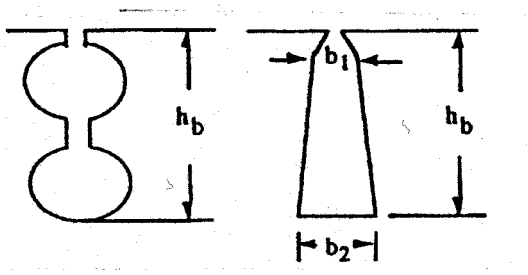

Fig. 3. Typical rotor slots for conventional induction machines.

where α is the ratio of harmonic and fundamental components. Each flux density is weighted by β. Since β is canceled in the ratios of flux densities, only the flux density in airgap is weighted by β. Thus a new function $F(\lambda)$ is defined as

$$F(\lambda) = \beta \cdot f(\lambda) \tag{6}$$

With this new function, the main dimensions of an induction machine can be obtained with both optimal proportions of iron and copper and taking into account the impact of the inverter.

On the other hand, maximum efficiency and improved power factor should be considered in (6) for an IDIM design because of the reasons stated in the above section. Thus, (3) will be utilized to determine the main dimensions of an IDIM by substituting $F(\lambda)$ for $f(\lambda)$.

In summary, even though the harmonics from an inverter may add negative impact on the IDIM, the end results of considering all of the factors brought by the inverter is that either the volume of the machine can be significantly reduced or the power rating can be increased.

B. Rotor Slot and Rotor Resistance

For a conventional induction machine, it is common to adopt a double cage or deep bars as shown in Fig. 3 to increase the skin effect for large rotor resistance during starting and high starting torque.

With skin effect considered, the effective rotor resistance follows the equation

$$r_r = \left[k_r \frac{l_e}{l_b} + \frac{l_b - l_e}{l_b}\right] r_b \tag{7}$$

where
r_b is the nominal rotor resistance without consideration of skin effect,
l_b the length of the rotor conductor,
l_e the effective length of the rotor core, and
k_r a coefficient accounting for skin effect.

Note that k_r is a function of slot factor as shown in Fig. 5. SF is defined as

$$\mathrm{SF} = 0.1987\, h_b \sqrt{\frac{b_b \cdot sf}{b_r \cdot \rho}} \tag{8}$$

where
h_b is the height of rotor conductor,
b_b the width of rotor conductor,
b_r the width of rotor slot,

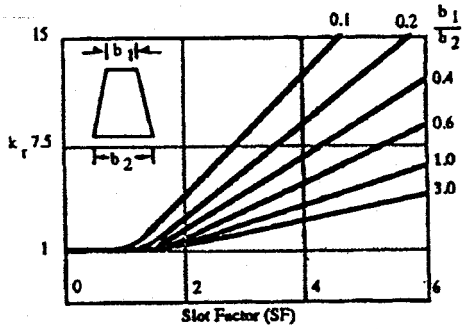

Fig. 4. Relationships of k_r to the slot factor (SF).

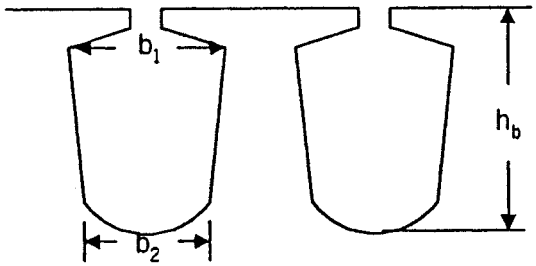

Fig. 5. Rotor slots suitable for inverter-driven induction machines.

sf the slip frequency, and

ρ the rotor conductor conductivity.

Basically, SF relates to slip frequency and the rotor slot height to the effective rotor resistance. As shown in Fig. 4, the ratio b_1/b_2 also affects k_i significantly.

In general, the deeper the rotor slot is and the higher the slip frequency is, the larger the SF and the effective rotor resistance will be. It is seen that the line-start requirement of a conventional induction machine will result in a large SF value. Another factor affecting SF is the required speed range at a fixed frequency. For a conventional induction machine operating in a range of 0.80–0.95 synchronous speed, the rotor slot area has to be larger than that with a small slip. A larger rotor slot is chosen to avoid excessive losses when the slip is higher.

Inspecting (7) and (8) and Fig. 4, it can be observed that the rotor slot in a conventional design is inevitably deeper and bigger than what actually is needed, if only the rated steady state operation is considered. As discussed previously, the inverter power supply is able to create such an operating condition so that even if the machine is continuously in a variable speed mode, it only experiences what the machine normally encountered in the rated steady state operation. Based on these considerations, an IDIM generally favors a shorter rotor slot shape with parallel teeth as shown in Fig. 5, which opposed to the deep bar or double cage shape. The ratio $b_1/b_2 > 1.0$ can also be realized.

As the results, the effective area of the rotor slot can be reduced by 15–25% from that of a conventional design without increasing the effective rotor resistance. In other words, the effective rotor resistance of an IDIM can be reduced by 15–25% while having the same area as that of conventionally designed rotor slots.

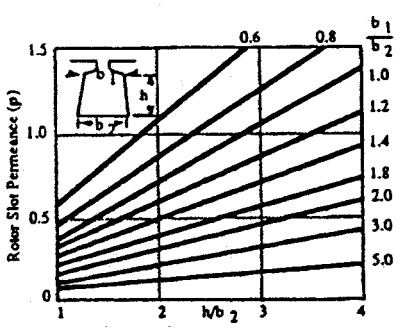

Fig. 6. Rotor leakage permeance vs. rotor slot shape.

C. Rotor Slot Leakage Reactance

As well known, rotor leakage reactance x_2 of an induction machine is proportional to the leakage permeance, ρ, determined by

$$x_2 = k \cdot \rho \tag{9}$$

Fig. 6 illustrates the relation of the rotor slot leakage permeance ρ to the shape of the rotor slot featured by h/b_2 and b_1/b_2. As can be observed from Fig. 3 (right figure), a deep slot ($h_b/b_2 > 2$) with a tip-up triangular shape ($b_1/b_2 < 0.6$) has a very large ρ and, thus, substantially increases the rotor leakage reactance.

With no considerations given to the starting characteristics, the rotor slot can be wider and shorter ($h/b_2 < 1.5$ and $b_1/b_2 > 0.9$) under the limitation of the flux density in rotor teeth. This reduces a much reduced rotor leakage reactance. A smaller rotor leakage reactance, in turn, contributes to an improved power factor and increased peak torque. Combined with the reduced rotor resistance, a small leakage reactance also helps to reduce the slip frequency for the rated torque, and reduce the slip frequency variation for a different torque level.

IV. Design, Analysis and Experimental Comparisons

The design strategies described in Section II and the alternatively interpreted design equations in Section III are implemented in a computer aided design package, IDIMCAD, which will be presented in another paper. In order to substantiate the proposed design strategies, the design, analysis and experimental results for IDIM's are presented in this section. Firstly, a family of parametric curves is generated to show the general merits of IDIM's. Then, the section will compare, experimentally, a conventional designed machine with a practical IDIM, which was designed by the IDIMCAD package. The comparison will highlight the improvement in rated output power and performance.

A. General Characteristics Estimation

In estimating the characteristics and computing the parameters of an induction machine designed with the discussed strategies, the following parametric curves are generated for a typical four pole induction machine under various levels of power ratings by the computer package:

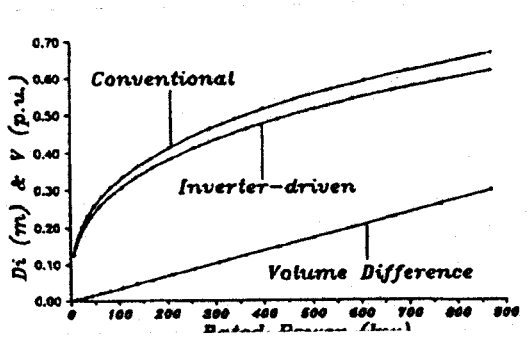

Fig. 7. Rotor outer diameter and volume reduction vs. power rating.

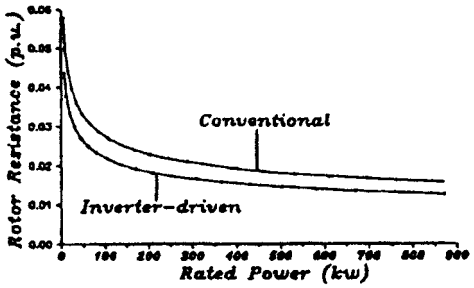

Fig. 8. Rotor resistance vs. power rating.

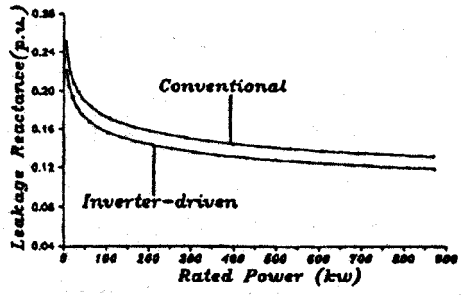

Fig. 9. Rotor leakage reactance vs. power rating.

1) Rotor Outer Diameters and Percentage of Volume Reductions versus the Power Rating: As can be seen clearly from Fig. 7, the rated power of an IDIM design is substantially larger than that of a conventionally designed machine for the same rotor size. In the figure, the percentage volume reduction is defined as

$$\Delta V = \frac{V_1 - V_2}{V_1} \times 100\% \tag{10}$$

where V_1 is the volume of the machine in conventional design, and V_2 that in inverter driven design. The figure also indicates that along with the increase of power rating, the percentage volume reduction gets larger. The benefits of designing a high power rating IDIM are evident.

2) Rotor Resistance and Leakage Reactance versus Power Ratings: As can be observed from Figs. 8 and 9, the rotor resistance and leakage reactance of an inverter driven machine design are smaller than those of a conventional design. The reduction in rotor resistance is especially evident when the power ratings are relatively low. The reduction in leakage reactance is independent of power ratings.

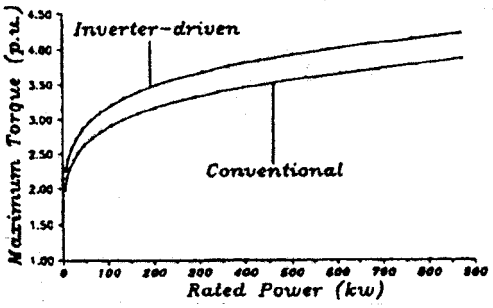

Fig. 10. Maximum torque vs. power rating.

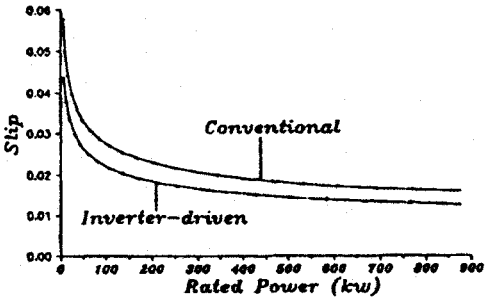

Fig. 11. Slip of the rated torque vs. power rating.

3) Maximum Torque versus Power Ratings: For a given voltage, the maximum torque is inversely proportional to the leakage reactance and winding resistance. The maximum torque of IDIM design is larger than that of a conventional one, and the improvement increases with the increase of the rated power as shown in Fig. 10.

4) Slip versus Power Ratings: In a similar way to the rotor resistance curve, the slip at the rated power of the inverter driven machine design is smaller than that of a conventional design as shown in Fig. 11. The reduction is more significant for low power ratings.

B. Experimental Comparisons

To further compare the difference between an inverter driven machine design and a conventional machine design, two induction machines are designed and tested with the same outer dimensions. Motor 1 is designed using the conventional method, and Motor 2 using proposed IDIM strategies implemented by the software IDIMCAD. The two machines' specifications are shown in Table I:

1) Design Results: Table II shows the major design results of the conventional (Motor 1) and the IDIM (Motor 2).

Fig. 12(a)–(b) show the dimensions and shapes of the rotor slots. Fig. 13 shows the external appearance of the Motor 2 with 15 kW power rating.

TABLE I
SPECIFICATIONS OF THE TWO MOTORS

	Output Power (kW)	Rated Voltage (Volt)	Syn. Speed (rpm)	No.of Pole	No.of Phase
Motor 1	11	380	1500	4	3
Motor 2	15	380	1500	4	3

TABLE II
COMPARISON OF DESIGN RESULTS

	Motor 1	Motor 2	Unit
Stator D_o/D_i	260 / 170	260 / 170	(mm)
Core length	150	150	(mm)
Airgap length	0.5	0.5	(mm)
Stator slot	44	48	
Rotor slot	36	38	
x_1/r_1	0.77 / 0.3126	0.71 / 0.3005	(Ω)
x_m	46.37	52.39	(Ω)
x_2/r_2	0.76 / 0.3111	0.63 / 0.2520	(Ω)
Stator /rotor iron	24.42 / 16.15	21.32 / 15.39	(kg)
Stator /rotor copper	10.67 / 6.53	12.85 / 7.01	(kg)

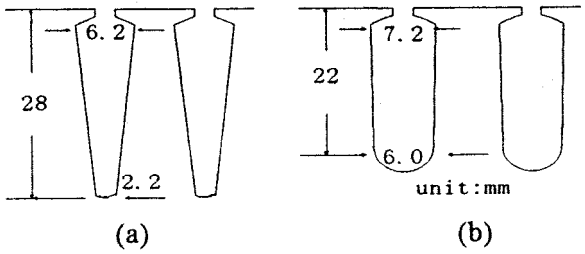

Fig. 12. Shapes of rotor slots of (a) Motor 1 and (b) Motor 2.

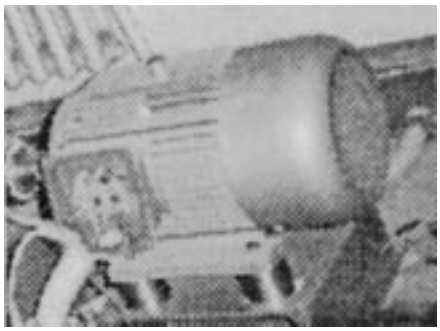

Fig. 13. The practical IDIM with 15 kW power rating.

As compared to Motor 1, Motor 2 has the same stator outer/inner diameters and effective length, but the stator slot number, rotor slot number, rotor slot dimensions and shape are noticeable different. The rotor slot depth of Motor 2 is decreased by about 20%, and the width increased by about 15%, resulting reduction of rotor resistance by 19% and rotor leakage inductance by 17%. In addition, the active iron and copper ratio and the numbers of stator and rotor slot in Motor 2

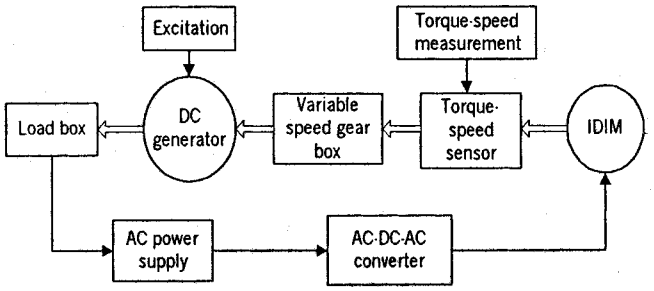

Fig. 14. The connection diagram of the test set.

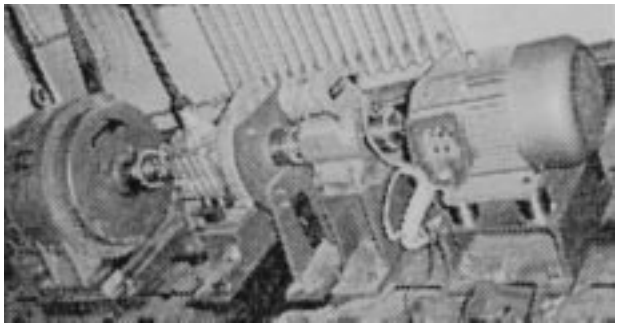

Fig. 15. Test site of Motor 2.

TABLE III
COMPARISON OF PERFORMANCES

	Motor 1	Motor 2	Unit
Rated input power	12	15	kW
Speed	1464	1465	Rpm
Phase voltage	220	220	Volts
Stator current	20.17	25.03	Amperes
Power factor	0.901	0.908	
Efficiency	92.2	91.8	%
Temperature rise	42.38	44.65	°C
T_{max} (at $V = V_n$)	181.6	218.87	N. m
T_s (at f = 5 Hz)	102	90	N. m
I_o (at V= Vn)	8.1	7.1	Amperes
I_s (at f = 5 Hz)	39.1	38.0	Amperes

are optimized based on the function $F(\lambda)$ for maximum output power.

2) Experiment Analysis: The practical test set consists of an IDIM, a torque-speed sensor, a variable speed gear box, a DC generator, a load box and a 25 KVA converter. The connection diagram is shown in Fig. 14 and the real test site is shown in Fig. 15.

Driven by the same inverter, the performance of Motor 1 and Motor 2 are tested and compared. Table III summarizes the results at their rated power, no-load and short-circuit operation conditions.

It is seen from Table III that at the rated point, the efficiency, power factor, temperature rise of the two motors are almost the same. However, the output power of Motor 2 is significantly 25% greater than that of Motor 1 and the maximum torque of Motor 2 is almost 1.2 times greater than that of Motor 1. The figures imply that if the two motors are designed same rated power, the size of Motor 2 will be about 25% smaller than that of Motor

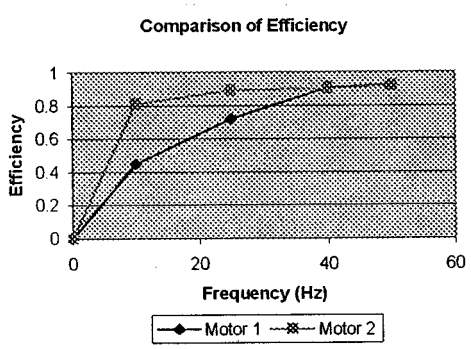

Fig. 16. Comparison of efficiency.

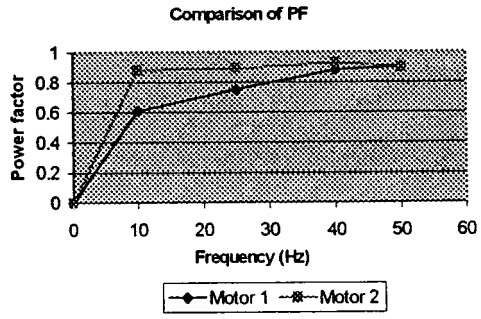

Fig. 17. Comparison of power factor.

1. In addition, the no-load current (I_o) of Motor 2 is about 13% smaller than that of Motor 1, which means that the passive power required by Motor 2 is less than that by Motor 1 due to larger x_m, and smaller x_2 in Motor 2. As to the start-up feature, the tests show that both Motor 1 and Motor 2 have enough capability to start up from standstill even at a very low frequency ($f = 5$ Hz).

Another comparison is done under constant torque condition, the two motors were tested for variable speed performance under varying input frequency. The results of the comparison are shown in Figs. 16 and 17 with a constant torque of 77 N.m.

Obviously, the efficiency and power factor of Motor 2 could be maintained at high values in a wide frequency range, while Motor 1 could achieve this only at the rated frequency. This is a major benefit from the proposed IDIM design strategies for variable speed systems.

V. Conclusion

The main goal of designing an IDIM is to realize an effective synergetic inverter/machine package for high performance and low cost variable speed systems. Based on the operating conditions of an inverter drive, alternative machine design strategies are proposed. Corresponding design equations are discussed and investigated. From the above design, analysis and experimental comparisons, we conclude that:

1) The main reason of having freedom to improve the IDIM design is that: the design is now independent of the restriction imposed by the line start-up performance requirements. The variable frequency provided by the inverter allows the design to be more focused on the performance in quasisteady state conditions and system optimization.
2) Overall size equations for inverter-driven induction machine design have to be changed, because only the most favorable operation conditions need to be considered.
3) Being freed from line-start requirement, the rotor slot number, shape, and size are to be reconsidered. The optimal design of rotor slots results in improved maximum torque, rated slip, and efficiency.
4) If an induction machine is designed in accordance with the above strategies and it is possible to increase output power by 20–30% without sacrificing the size and performance.

References

[1] R. H. Daugherty and C. U. Wennerstrom, "Need for industry standards for AC induction motors intended for use with adjustable-frequency controllers," *IEEE Trans. on Industry Applications*, vol. 27, pp. 1175–1185, Nov./Dec. 1991.

[2] N. P. Nee and C. Sadarangani, "The influence of load and rotor slot design on harmonic losses of inverter-fed induction motors," in *Proceedings of IEE Electrical Machine and Drives Conference*, Sept. 1993, pp. 173–178.

[3] N. P. Nee, "Rotor slot design of inverter-fed induction motors," in *Proceedings of IEE Electrical Machines and Drives Conference*, Sept. 1995, pp. 52–56.

[4] Y. Akiyama *et al.*, "A study of the most suitable design of inverter-driven induction motors," *PCIM*, pp. 38–44, June 1994.

[5] Z. M. Zhao, L. Y. Xu, and A. El-Antably, "Strategies and a computer aided package for design and analysis of induction machines for inverter-driven variable speed systems," in *Proceedings of IEEE IAS Annual Meeting*, Oct. 1995, pp. 523–529.

[6] S. Williamson and C. I. McClay, "Optimization of the geometry of closed rotor slot for cage induction motors," *IEEE Trans. on Industry Applications*, vol. 32, no. 3, pp. 560–568, May/June 1996.

[7] A. Barbour and W. T. Thomson, "Finite element study of rotor slot designs with respect to current monitoring for detecting static airgap eccentricity in squirrel-cage induction motors," in *Proceedings of IEEE IAS Annual Meeting*, Oct. 1997, pp. 112–119.

[8] K. Matsuse *et al.*, "Analysis of inverter-fed high speed induction motor considering skew factor and crosspath resistance between adjacent rotor bars for wide speed range," in *Proceedings of IEEE IAS Annual Meeting*, Oct. 1996, pp. 618–624.

[9] S. Chen and S. N. Yen, "Optimal efficiency analysis of induction motors fed by variable-voltage and variable frequency source," *IEEE Trans. on Energy Conversion*, vol. 7, pp. 537–543, Sept. 1992.

[10] V. B. Honsinger, "Sizing equations for electrical machinery," *IEEE Trans. on Energy Conversion*, vol. 2, no. 1, pp. 116–121, Mar. 1987.

Z. M. Zhao received the B.S. and M.S. degrees from Hunan University in 1982 and 1985 respectively, the Ph.D. degree from Tsinghua University, PR China in 1991, all in electrical engineering. He is now a Professor in the Department of Electrical Engineering, Tsinghua University. He was a Postdoctoral Fellow in the Ohio State University of U.S.A in 1994–1996, and worked in the University of California at Irvine as a Visiting Scholar in 1996–1997. He had an academic stay in The University of British Columbia and The Hong Kong University as a Visiting Professor in 1998 and 1999, respectively. His areas of interest include parameter identification and modeling, power electronics and motor drive, and design, analysis and control of electric machines.

S. Meng received the B.S. degree from Tsinghua University in 1996, and is currently pursuing the Ph.D. degree in Tsinghua University. His interests include the design and modeling of electric machinery and electric drive system.

C. C. Chan started his professional electrical engineering career in 1959. He worked 11 years in industry and 25 years in academic institutions. He is now a Full Professor in the Department of Electrical and Electronic Engineering, University of Hong Kong, and the Director of the International Research Center for Electric Vehicles. He was elected Fellow of the IEEE for his contributions to the advancement of electric drives and electric vehicles. He is also a Fellow of IEE and HKIE and Chairman of an IEEE Technical Committee. He is co-founder of the World Electric Vehicle Association.

E. W. C. Lo obtained his B.S., M.S., and Ph.D. degrees all from the Electrical and Electronic Department of the University Hong Kong. He has years of industrial experience in areas of electrical installation and energy management, and he has held research and teaching positions in a number of tertiary institutions before he joined the University of Hong Kong in 1995. He serves as a Consultant for a number of industrial organizations. His research interests are generally the electrical services in buildings, as well as, control of electric drive systems.